

IMPROVED METHODS FOR REGIONALIZED SURFACE WAVE ANALYSIS

Jeffrey L. Stevens and David A. Adams, Maxwell Technologies, Systems Division

Sponsored by U. S. Department of Defense
Defense Threat Reduction Agency
Contract No. DSWA01-98-C-0154

ABSTRACT

The goal of this project is to improve the capability to identify and detect surface waves under a Comprehensive Nuclear-Test-Ban Treaty. This is accomplished through the following tasks: improvement of regionalized station magnitudes through development of improved regionalized phase and group velocity models and other parameters, development of regionalized path-corrected spectral magnitudes, and improvement of automated surface wave detection using phase-matched filtering; development of maximum likelihood network spectral magnitudes and magnitude upper bounds; and optimization of the Ms:mb discriminant using both time domain and spectral magnitudes.

The first objective is to improve the dispersion curves, which are now in use at the International Data Centre (IDC) and were developed in a previous project. The global dispersion data set has been expanded by about 50% and now contains over 164,000 data points including; Eurasian, Antarctic, and South American group velocity measurements from Levshin and Ritzwoller (University of Colorado), phase and group velocity measurements from the Middle East and Saudi Arabia (Herrmann, Mitchell, and Mokhtar at St. Louis University), a model of global low-frequency phase velocities, dispersion curves from historic explosion data sets, and a large number of measurements made from prototype International Data Centre data (Maxwell Technologies). This expanded data set provides extensive coverage of the Middle East and Saudi Arabia, and fills in some important gaps, such as Antarctica, which were poorly constrained in the earlier data set.

This data set is used to perform a global tomographic inversion, which determines the shear velocity as a function of depth in approximately 150 discrete earth models. These earth models are then used to calculate phase and group velocity curves, which are used in automatic detection and identification of surface waves. The current automatic processing system in place at the IDC uses narrow-band filtering to determine group velocities, which are then compared with the predicted group velocities for the path. We expect to be able to replace this with a more robust method based on phase-matched filtering using the improved phase velocity dispersion curves. The earth models are also used to develop path-corrected spectral magnitudes, a type of moment, to regionalize the surface-wave excitation functions as well as surface-wave dispersion.

Key Words: surface wave, dispersion curve, phase matched filter, regionalization, moment

Processing of auxiliary long-period data may be added in the future. Surface waves are processed for all stations within 100 degrees of each event. The PIDC/IDC processing procedures are summarized here, and are described in detail by Stevens and McLaughlin (1999).

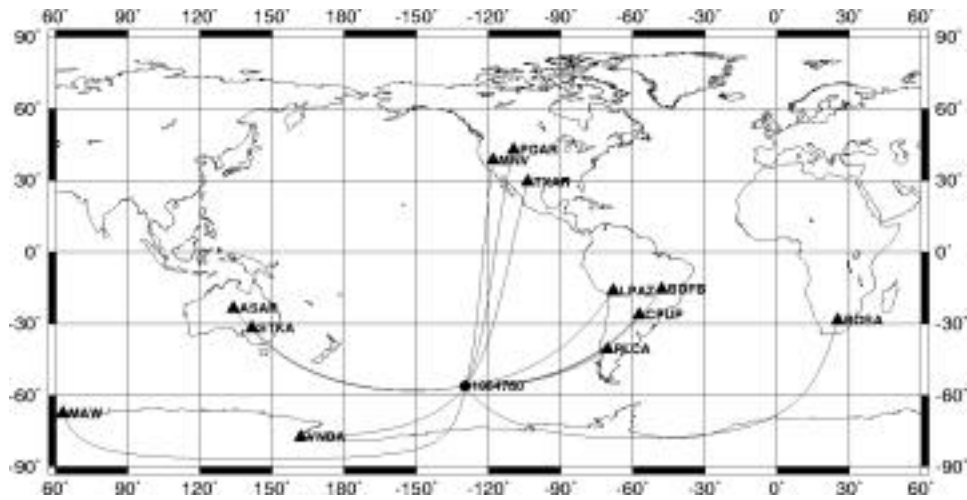


Figure 2. Map showing location of a 1997 South Pacific earthquake and the 12 IMS stations within 100 degrees that recorded the event. Lines are great circle paths.

Maxsurf runs in the processing stream after events have been identified and located. Maxsurf then examines the arrival window where a surface wave would be expected and applies a dispersion test to see if a surface wave can be identified. If so, then the amplitude is measured and stored in the IDC database. We start with an example that illustrates this procedure. Figure 2 shows the location of an m_b 3.9 South Pacific earthquake that occurred on 1997 June 15, together with the 12 IMS stations within 100 degrees that recorded the event, and the great circle paths between the earthquake and the stations.

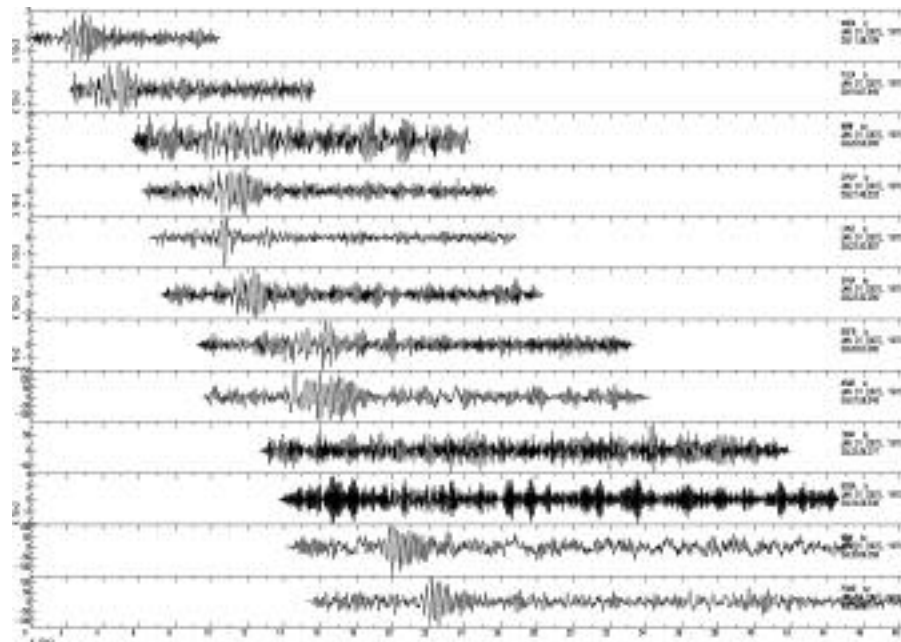


Figure 3. Long period data from the 1997 South Pacific earthquake. Seismograms are ordered by distance from the earthquake. All seismograms have been transformed to a common KS36000 instrument.

Figure 3 shows the data recorded at these stations after conversion to a common (KS36000) instrument. The surface wave is visible at most of the stations, however it is obscured by noise and difficult to see at some of them. Surface

waves are identified in the following way: a set of narrow band filters are applied to the data over a set of 8 frequencies from 0.02 to 0.06 Hz. A long-period or broadband beam is formed at arrays with the expected azimuth and slowness. The arrival times at each frequency are then compared with predicted arrival times generated from the regionalized group velocity model which will be described later in this paper. Figure 4 shows the bounds on the allowed dispersion and the measured group velocities at the 8 frequencies for several stations. The dispersion test requires that 6 of the 8 measured data points lie within the predicted bounds, and all stations except for TXAR pass this test. The marginal data fit at VNDA is due to inaccuracies in the model near Antarctica. The fit is improved significantly by the more recent models discussed later in this paper.

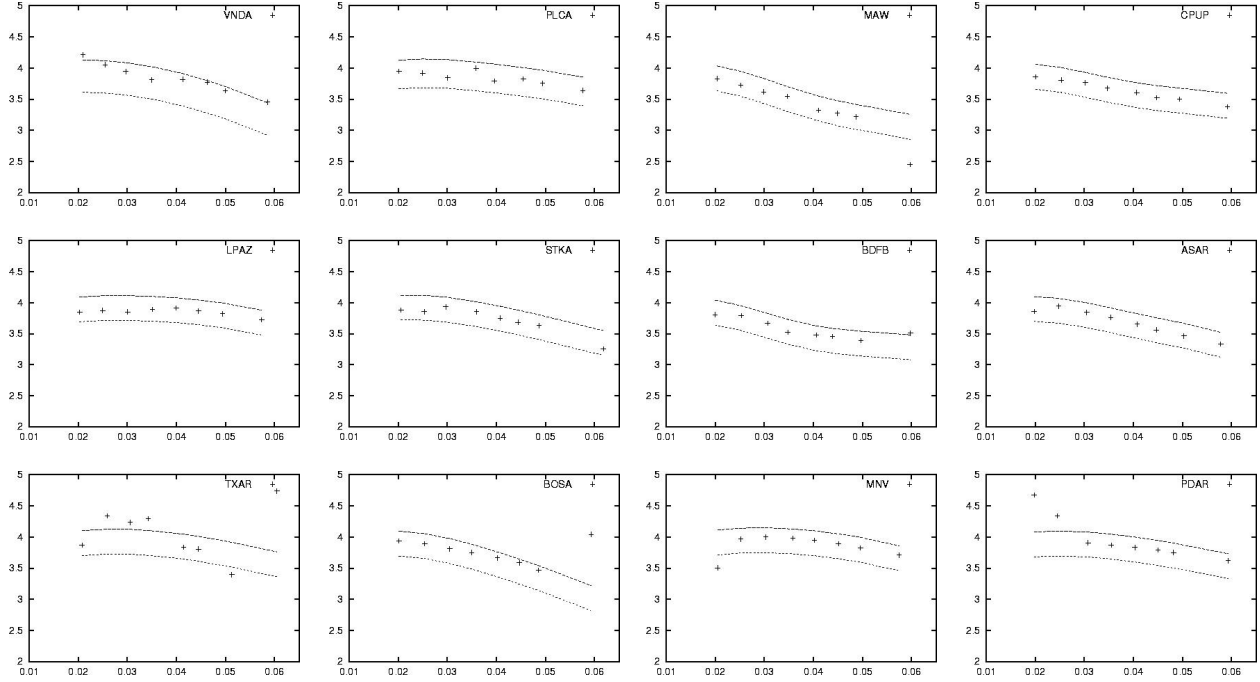


Figure 4. Measurements of group velocity made by narrow band filtering of the seismograms in Figure 3, and the predicted dispersion window. Plus signs indicate measured data. Lines indicate the predicted dispersion curve offset above and below to determine the allowable time window as discussed in the text. The dispersion curves are ordered by increasing source to receiver distance.

Optimization of Surface Wave Processing and Analysis

Surface wave processing can be optimized by defining a path corrected spectral magnitude which can be regionalized to allow for geographic variations in source excitation, attenuation, and dispersion, and can also be measured at different frequency bands in order to optimize signal to noise ratio. To do this, we base the magnitude on the equation for surface waves in a plane-layered structure. This equation can be factored into functions that depend on the source and receiver earth structure and the phase velocity and attenuation integrated over the path. The displacement spectrum for a Rayleigh wave at distance r from an *explosion* is given by:

$$U(\omega, r) = M_0' \frac{S_1^x(\omega, h_x) S_2(\omega) \exp[-\gamma_p(\omega) r + i(\varphi_0 - \omega r / c_p(\omega))]}{\sqrt{a_e \sin(r / a_e)}} \quad (1)$$

S_1^x depends on the source region elastic structure and the explosion source depth. S_2 depends on the receiver region elastic structure, γ_p is the attenuation coefficient that depends on the attenuation integrated over the path between the source and receiver. c_p is the phase velocity integrated over the source to receiver path. φ_0 is the initial phase of the source. a_e is the radius of the earth. $M_0' = \frac{3\beta^2}{\alpha^2} M_0$ where M_0 is the explosion isotropic moment. This definition is introduced so that the function S_1^x does not depend explicitly on the material properties at the source depth.

We can use Equation 1 to define a spectral magnitude corrected for distance and spectral shape. We define, for any event, earthquake or explosion, the scalar moment (Stevens, 1986):

$$M'_0 = \left| U(\omega, r, \theta) \frac{S_1^x(\omega, h_x) S_2(\omega) \exp[-\gamma_p(\omega)r + i(\varphi_0 - \omega r / c_p(\omega))]}{\sqrt{a_e} \sin(r / a_e)} \right| \quad (2)$$

$\log M'_0$ is then a path corrected spectral magnitude that can be evaluated over any desired frequency band. This is similar to the approach taken by Okal and Talandier (1987) in defining a mantle magnitude M_m , except that they used an averaged earthquake source spectrum that they referred to as the Rayleigh Wave “Excitability” instead of the explosion excitation function S_1^x at the reference depth h_x . Although the imaginary part of the exponential is removed by the absolute value, it is shown here explicitly because in practice the phase is used to generate a phase-matched filter (Herrin and Goforth, 1977) to compress the signal and improve signal/noise ratio prior to taking the spectrum. The spectrum is then averaged over a frequency band to smooth the spectrum and obtain a stable measurement.

For an isotropic explosion source at depth h_x , M'_0 is independent of frequency. Equation 2 therefore corrects completely for all frequency dependent and distance dependent factors in the observed spectrum. In general, M'_0 for an earthquake is not completely frequency independent, but it is partially corrected for frequency dependence by removal of the path attenuation and receiver structure and similarities in the explosion and earthquake excitation functions in the same source region. The remaining differences mean that the earthquake magnitude will vary somewhat when measured over different frequency bands while the explosion will not. In particular, the spectra of deeper earthquakes will decline more rapidly with increasing frequency, while the path corrected spectra of shallow earthquakes is approximately flat over the frequency band of about 0.01-0.08 Hz.

By defining the path corrected spectral magnitude as the logarithm of Equation 2, we obtain a measure of surface wave magnitude that is independent of range, nearly independent of frequency, and regionalizeable. The functions S_1^x and S_2 depend only on the source and receiver points and can be stored in a simple lookup table. The functions γ_p and c_p depend on the source to receiver path and can be found by integrating along a great circle path between the source and receiver in a regionalized earth model.

Development of Regionalized Earth Models

With a set of regionalized earth models that maps any point on the earth into the earth structure at that point, we can calculate all of the quantities in Equation 4 for any source and receiver point and calculate the path corrected spectral magnitude from any observed seismogram. In addition, we can use the phase velocity for the path to construct phase matched filters, and use the predicted group velocity arrival times as part of an existence test for surface waves in automatic processing as discussed earlier.

Observed surface waves provide strong constraints on earth structure, so development of regionalized earth models can be a self-correcting process. That is, surface wave dispersion and amplitudes can be used to infer earth structure, and earth structure can be used to calculate surface wave dispersion and amplitudes. So with a data center such as the IDC which collects surface wave data on a continuous basis, it is possible to implement a program of continuous improvements in regionalization and surface wave processing using this extensive data set. In the following, we have used dispersion data measured from GSETT3 PIDC data, merged with dispersion data from other studies to develop regionalized global earth models.

Stevens and McLaughlin (1999) describe development of the global earth model with 149 distinct models on a five degree grid that is now used for surface wave identification at the PIDC and IDC. The development used global tomographic inversion of about 90,000 dispersion measurements, using the Crust 5.1 model (Mooney, et al., 1998) as a starting point. We have continued this process further, adding more data points and additional models. The global dispersion data set now contains over 164,000 data points including:

Global surface wave group velocities from earthquakes derived using PIDC GSETT3 data (Stevens and McLaughlin, 1996), augmented with more recent measurements derived from PIDC data.

1. Surface wave phase and group velocity dispersion curves from underground nuclear test sites (Stevens, 1986; Stevens and McLaughlin, 1988), calculated from earth models for 270 paths (test site – station combinations) at 10 frequencies between 0.015 and 0.06 Hz.
2. Phase and group velocity measurements for western Asia and Saudi Arabia from Mitchell et al.(1996) for 12 paths at 17 frequencies between 0.012 and 0.14 Hz.
3. Global phase velocity model of Ekstrom et al. (1996) for 9 periods between 35 and 150 seconds calculated for each 5 degree grid block from a spherical harmonic expansion of order $l=40$.
4. Group velocity measurements for Eurasia from Ritzwoller et al.(1996) and Levshin et al.(1996) for 20 frequencies between 0.004 and 0.1 Hz with 500 to 5000 paths per frequency.
5. Antarctic and South American group velocity measurements from the University of Colorado (Vdovin et al., 1999; Ritzwoller et al., 1999).
6. A very large set of dispersion measurements from Saudi Arabia provided by Herrmann and Mokhtar at St. Louis University.

This expanded data set provides extensive coverage of the middle east and Saudi Arabia, and fills in some important gaps, such as Antarctica, which were poorly constrained in the earlier data set.

The new shear velocity models obtained by tomographic inversion of this data set are changed primarily in areas that contain additional data. For example, there is now more variation in the shear velocity structure in the Arabian plateau where high frequency dispersion data provides additional information about this structure. This is a good test showing both that the tomographic inversion is responding correctly to new data, and that the previous inversion was stable with respect to the addition of new data in other regions. The current IDC model and the model discussed above as well as calculated dispersion curves and other quantities may be downloaded from the World Wide Web at: http://www.maxwell.com/products/geop/PAGEOPH_CTBT/SurfWave/LP_export.html. We have reviewed the results of this inversion, and are trying to find the optimum ways to improve the results further. What we are trying to find are a set of models that accurately predict the phase and group velocity dispersion, and ultimately the amplitude, for any source and receiver point. There are three basic ways to improve the inversion results, depending on what is causing the inaccuracy in the current model. These are:

1. Add additional model types. The inversion described above, as well as the current IDC models, use 149 distinct models, and each model corresponds to a number of locations in the world with similar crustal types. However, as the data set becomes more complete, and it becomes possible to resolve differences between the same model in different locations, it is necessary to subdivide some of these regions. At some point, we expect to divide the regions into smaller blocks than the current 5 degree grid.
2. Add additional model layers. The current set of models contain only a few layers in the crust, similar in most cases to the Crust 5.1 models that were the starting point for the initial set of inversions. As we get more higher frequency data, we develop additional resolving power in the crust, and it will be necessary to add more layers and allow more variation in the crust.
3. Add new data to fill in gaps. The first two changes above are for regions where there is an abundance of data. However, we still have some regions where the data is limited and may not be adequate to constrain the models sufficiently. In these regions, we need to find additional dispersion data to add to the data set.

We want to accomplish 1 and 2 above without adding new models and layers that do not contribute to improvements in the data fit. We therefore tried to find ways to identify those regions that could not be modeled well with the existing 149 models. We did this in three ways:

1. We identified outliers in the data and plotted the corresponding ray paths color coded according the residuals, to identify poorly modeled regions.

2. We identified clusters of similar ray paths. Such clusters can be used to check the robustness of outlying data. Clusters that have consistently anomalous residuals can be used to make routine path corrections, once a final model is determined.
3. We performed tomographic inversions for specific frequency ranges. The 2D group velocity tomographic inversions were done for 8 frequency bands:- below 0.01 Hz, 0.01 to 0.0167 Hz, 0.0167 to 0.025 Hz, 0.025 to 0.033 Hz, 0.033 to 0.04 Hz, 0.04 to 0.05 Hz, 0.05 to 0.067 Hz, and greater than 0.067 Hz. The inversions were done without smoothing or damping. We selected 84 cells with changes of more than 3% in group velocities and occurring with the same sign at more than two adjacent frequency bands, and with more than 15 ray paths intersecting. From these 84 cells, we found 3 pairs of adjoining cells with similar velocity changes. We associated a single new model type for each pair, thus reducing the total number of new model types to 81. Figure 5 shows the locations of the 84 cells colored coded depending on the change in group slowness for the frequency band 0.025 to 0.033 Hz. The initial structures of each of these 81 cells were the same as the original model types, however they were allowed to adjust independently of the original models during the following shear wave velocity tomography.

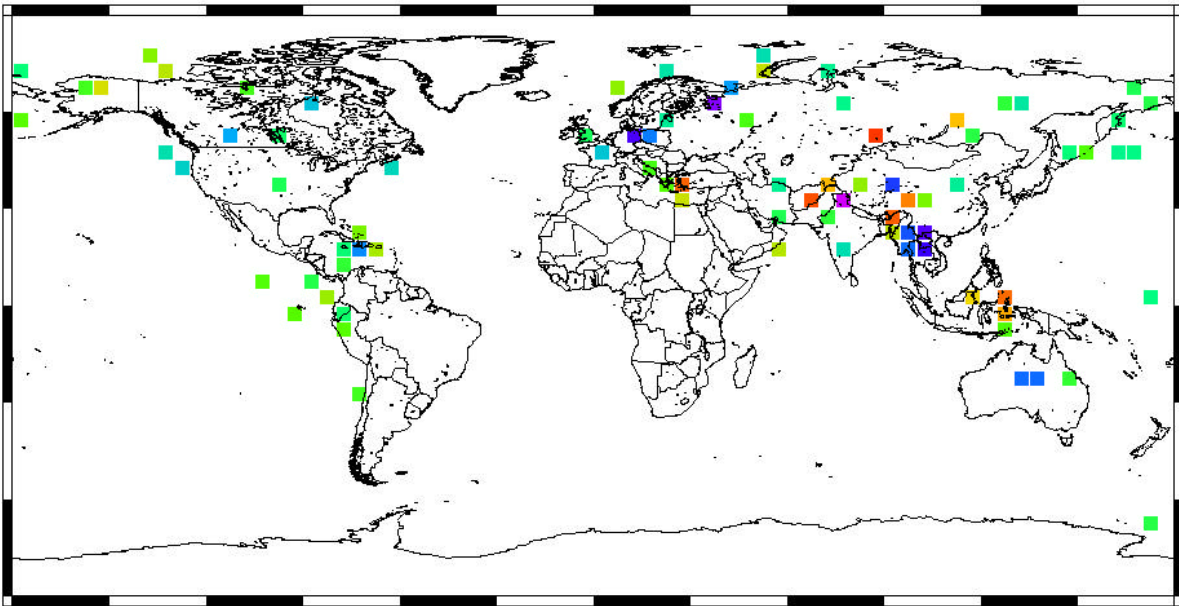


Figure 5. New models added to surface wave tomographic inversion.

This increased the total number of model types from 149 to 230. This reduced the total data variance by about 4%. This relatively small variance reduction reflects the fact that the initial model fit the data quite well over most of the world, and that the improvements occur primarily in the limited regions illustrated in Figure 5. The improvement in data fit is more substantial in these regions

Path Corrected Spectral Magnitudes and Phase-matched Filtering

A second automatic surface wave processing program, Maxpmf, has been developed which is similar to Maxsurf except that it applies phase-matched filtering to seismograms and calculates path-corrected spectral magnitudes in addition to M_s . Maxpmf integrates a regionalized phase velocity model to generate a phase-matched filter and applies amplitude corrections to generate a path-corrected spectral magnitude ($\log M_0$). An advantage of the frequency domain processing is that a spectral magnitude of either signal or noise can always be measured over the specified frequency band, while it may not be possible to measure data in a specified frequency band in the time domain. Maxsurf, for example, will reject a seismogram if it can't find a 20 second arrival within the predicted arrival time window. This often occurs at regional distances and there is no reason for such a restriction for spectral magnitudes. Consequently, moments can be measured for regional seismograms in cases where standard M_s measurements cannot be made.

Figure 6 shows an example of phase-matched filtering derived from the regional phase velocity model applied to the data set discussed earlier and shown in Figure 3. The surface waves are compressed into a narrow time window near zero and amplified relative to the noise.

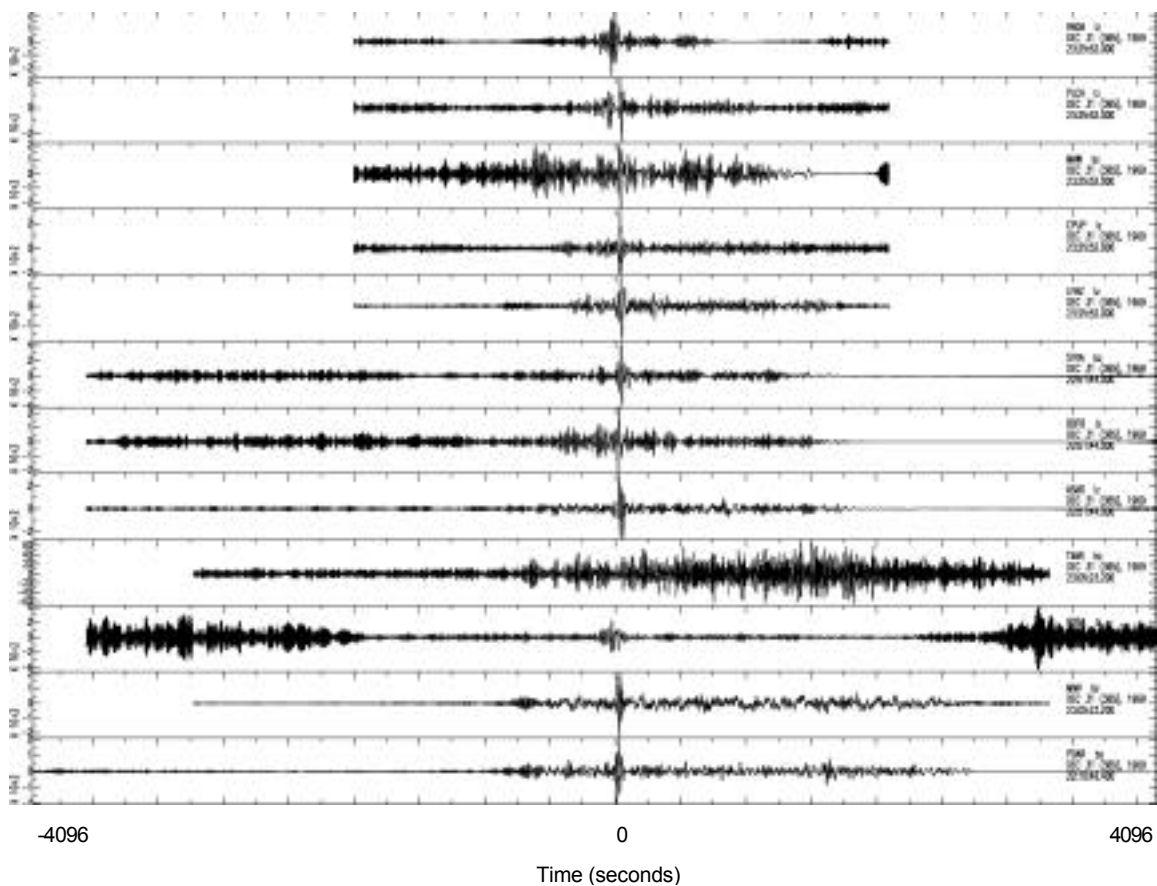


Figure 6. Waveforms from Figure 3 after phase-matched filtering. The surface wave is compressed into a narrow time window near zero.

One of the goals of the current project is to use phase-matched filtering directly for surface wave identification rather than performing narrow-band filtering first, and then using phase-matched filtering for measurement. As can be seen in Figure 6, the improvement in signal to noise ratio derived from phase-matched filtering suggests that the detection threshold could be reduced by eliminating the narrow-band filtering step. However, the narrow-band filter detection procedure now in place has been tested carefully and is mature enough that spurious or incorrect identification of arrivals is relatively rare, so replacement with an alternative procedure requires extensive testing to ensure that improvement in detection does not come at the expense of erroneous detection. We have started this process by running phase-matched filters in a semi-operational mode on PIDC data. We ran Maxpmf on two days of continuous data (approximately 650 waveforms within the correct time and distance windows), and saved a number of parameters from phase-matched filtering. We looked first to see if the signal enhancement alone was sufficient to identify surface waves. That is, we looked at the rms amplitude in the region near zero time, and compared it with the rms amplitude over a longer time window outside of this region. We found that this did, in fact, identify a substantial fraction of the surface waves identified by narrow band filtering, however it is not as reliable and has a higher error rate. We are now investigating narrow-band filtering of the compressed waveform as a potentially more robust method of identifying surface waves in the compressed and enhanced signal.

CONCLUSIONS AND RECOMMENDATIONS

In this paper, we have described procedures for optimization of surface wave processing under a Comprehensive Test Ban Treaty, and described improvements to regionalized dispersion models and phase-matched filtering that are necessary for their implementation. Because the number of events increases rapidly at small magnitudes, a decrease

in the threshold of reliable surface wave detection and measurement can greatly reduce the number of unidentified events. Improved surface wave analysis methods can reduce the surface wave magnitude threshold, improve screening capability, and reduce the likelihood of unnecessary on-site inspections under a CTBT. We are continuing to improve the regionalized models, and to test and implement surface wave identification using phase-matched filtering to reduce the threshold for surface wave identification and measurement further.

ACKNOWLEDGEMENTS

We would like to thank Mike Ritzwoller and Anatoli Levshin of the University of Colorado, Brian Mitchell and Bob Herrmann of St. Louis University, Goran Ekstrom of Harvard University, and their coworkers for the use of their data and models in this project. We thank Keith McLaughlin, Mike Skov and Hans Israelsson for their help in development of these techniques and implementation and testing of this work at the PIDC.

REFERENCES

- Ekstrom, G., A. M. Dziewonski, G. P. Smith, and W. Su (1996), "Elastic and Inelastic Structure Beneath Eurasia," in *Proceedings of the 18th Annual Seismic Research Symposium on Monitoring a Comprehensive Test Ban Treaty, 4-6 September, 1996*, Phillips Laboratory Report PL-TR-96-2153, July, pp. 309-318, ADA313692.
- Fisk, M. D., D. Jepsen, and J. R. Murphy (1999), "Experimental Event-Screening Criteria at the Prototype International Data Center," submitted to *Pure and Applied Geophysics*.
- Herrin, E. and T. Goforth (1977), "Phase-Matched Filtering: Application to the Study of Rayleigh Waves," *Bull. Seism. Soc. Am.*, v. 67, pp. 1259-1275.
- Levshin, A. L., M. H. Ritzwoller, and S. S. Smith (1996), "Group Velocity Variations Across Eurasia," in *Proceedings of the 18th Annual Seismic Research Symposium on Monitoring A Comprehensive Test Ban Treaty, 4-6 September, 1996*, Phillips Laboratory Report PL-TR-96-2153, July, pp. 70-79, ADA313692.
- Mitchell, B. J., L. Cong and J. Xie, (1996), "Seismic Attenuation Studies in the Middle East and Southern Asia", St. Louis University Scientific Report No. 1, PL-TR-96-2154, ADA317387.
- Mooney, W., G. Laske, and G. Masters (1998), "Crust 5.1: A Global Crustal Model at 5x5 Degrees," *Journal of Geophysical Research*, v. 103, no. B1, pp. 727-747.
- Okal, E. A. and J. Talandier (1987), "M_m: Theory of A Variable-Period Mantle Magnitude," *Geophysical Research Letters*, v. 14, pp. 836-839.
- Ritzwoller, M. H., A. L. Levshin, L. I. Ratnikova, and D. M. Tremblay (1996), "High Resolution Group Velocity Variations Across Central Asia," in *Proceedings of the 18th Annual Seismic Research Symposium On Monitoring A Comprehensive Test Ban Treaty, 4-6 September, 1996*, Phillips Laboratory Report PL-TR-96-2153, July, pp. 98-107, ADA313692.
- Ritzwoller, M.H., O.Y Vdovin, and A.L. Levshin (1999), "Surface wave dispersion across Antarctica: A first look", *Antarctic J. U.S.*, in press.
- Stevens, J. L. (1986), "Estimation of Scalar Moments From Explosion-Generated Surface Waves," *Bull. Seism. Soc. Am.*, v. 76, pp. 123-151.
- Stevens, J. L. and K. L. McLaughlin (1996), "Regionalized Maximum Likelihood Surface Wave Analysis," Maxwell Technologies Technical Report submitted to Phillips Laboratory, PL-TR-96-2273, SSS-DTR-96-15562, September, ADA321813.
- Stevens, J. L. and K. L. McLaughlin (1999), "Optimization of surface wave identification and measurement," submitted to *Pure and Applied Geophysics*.
- Vdovin, O. Y., J. A. Rial, M. H. Ritzwoller, and A. L. Levshin, 1999, "Group-velocity tomography of South America and the surrounding oceans", *Geophys. J. Int.*, 136, 324-330.